# Daytime site characterisation of La Palma, and its relation to nighttime conditions

Matthew J. Townson[a], Aglaé Kellerer[a], James Osborn[a], Timothy Butterley[a], Timothy Morris[a], Richard W. Wilson[a]

[a]Department of Physics, Durham University, South Road, DH1 3LE, England;

July 10, 2014

## ABSTRACT

This paper presents preliminary daytime profiles taken using a Wide-Field Shack-Hartmann Sensor at the Swedish Solar Telescope (SST), La Palma. These are contrasted against Stereo-SCIDAR data from corresponding nights to assess the validity of the assumptions currently used for simulating the performances of possible Multi-Conjugate Adaptive Optics (MCAO) systems for future solar telescopes, especially the assumption that the structure of the high altitude turbulence is mostly similar between the day and the night. We find that for our data both the altitude and the strength of the turbulence differ between the day and the night, although more data is required to draw any conclusions about typical behaviour and conditions.

**Keywords:** instrumentation, site testing, atmospheric profiles, solar astronomy, S-DIMM+, SCIDAR, SLODAR.

## 1. INTRODUCTION

Current site testing studies for the locations of the next generation of large solar telescopes largely look at the integrated seeing value for the atmosphere, and profiles which have been taken are high resolution, low altitude profiles for the Advanced Technology Solar Telescope (ATST).[1] This will give the locations which give the best performance for a conventional Ground Layer Adaptive Optics (GLAO) assisted telescope. However the planned large solar telescopes are to be fitted with MCAO in order to increase their usable field of view. These systems correct the ground layer turbulence as well as number of other layers at higher altitudes.

The performance of an MCAO system is dependant on the height distribution of the turbulence, and not just on the value of the integrated seeing.[2] This makes it crucial to know if the current assumptions used for simulating profiles of the atmosphere in the daytime are correct for site selection, as well as having some way of monitoring the structure of the atmosphere while an MCAO system is running in a layer-oriented mode.

Simulations of the performance of these MCAO systems rely on knowledge of the structure of the atmosphere from nighttime profiles from instruments such as SLODAR[3] and SCIDAR,[4] despite the large discrepancy between the integrated seeing measurements of these instruments and those measured at the sites in the day.[5] This is taken into account by using ground layer information acquired during the day, and assuming that the structure of the high layer turbulence is similar between night and day.[6]

Data was gathered on La Palma on 19th September 2013 with a Wide-Field Wave-front Sensor (WF-WFS), similar to the one used on S-DIMM+,[7] also situated on La Palma. The data was then reduced using a SLODAR style analysis to calculate full atmospheric profiles for the site. This is especially important as the European Solar Telescope (EST) is to be situated in the Canary Islands, possibly La Palma,[8] and is due to have an MCAO system in order to achieve high resolution across the whole field of view ($2 \times 2\mathrm{arcmin}^2$).

Email: matthew.townson@durham.ac.uk

Ground-based and Airborne Instrumentation for Astronomy V, edited by Suzanne K. Ramsay, Ian S. McLean, Hideki Takami, Proc. of SPIE Vol. 9147, 91473E · © 2014 SPIE · CCC code: 0277-786X/14/$18 · doi: 10.1117/12.2056451

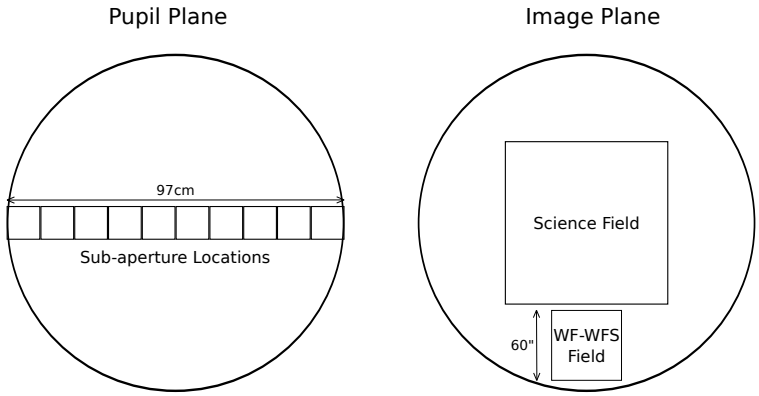


Figure 1. The diagram on the left shows the locations of the sub-apertures used across the pupil. A single row of sub-apertures, which were aligned horizontally with respect to the optical bench was used. This gave the maximal number of baselines in sub-apertures across one dimension, but also decreased the size of the images on the detector to allow for faster readout times, and reduced file sizes. The diagram on the right shows the image plane of the SST where a field stop was placed for the science field, and a small pickoff for the WF-WFS.

## 2. METHOD

The instruments which were used to gather profiles were a WF-WFS (sec. 2.1), as used by S-DIMM+[7] and Stereo-SCIDAR[9] for daytime and nighttime profiles respectively. These instruments were both situated on La Palma on the 18th and 19th September 2013. The WF-WFS was placed on the SST, and the Stereo-SCIDAR on the Jacobus Kapteyn Telescope (JKT). The profiles from the night of the 18th September are given in Sec. 3.1, with the daytime profiles for the 19th September given in Sec. 3.2. Poor seeing conditions limited the amount daytime profile measurements that could be made, so the daytime data set is much smaller than the night time one.

### 2.1 Wide-Field Wavefront Sensor

The WF-WFS used in this campaign was a slightly modified S-DIMM+.[7] The optical components used were identical, but the camera was replaced with a larger size CMOS chip. The WF-WFS was run taking data for a single row of sub-apertures running across the pupil in order to increase the working frame rate to 100Hz. The instrument field of view and sub-aperture arrangement on the telescope pupil is shown in fig 1.

The instrument relies on tracking the motions of solar granules, so if the conditions are such that it is not possible to distinguish the solar granulation, it is not possible to reconstruct profiles. This does not pose a problem in general for measuring profiles, as when the conditions are bad enough to stop the tracking algorithms from working properly, the data is also far too poor for any Adaptive Optics (AO) to work, or for any useful science data to be taken.

Profiles are generated from the images taken in each of the sub-apertures by comparing the statistics of the granular motion of different parts of the solar image, through the different lines of sight they trace out through the atmosphere. It is possible to then triangulate the altitude where the perturbations are coming from, as well as their strength from where these lines of sight overlap, which is described in fig 2.

A sample image from the WF-WFS is shown in fig 3. The size of the pickoff for the WF-WFS acts as a field stop, preventing the different sub-aperture images from overlapping. The large field of view in each of the sub-apertures allows for many different directions on sky to be observed simultaneously, giving a good altitude resolution to the instrument.

The global tip/tilt is removed from the WF-WFS in order to remove the effects of telescope tracking errors and image shake in software, post image capture. These motions appear on all of the sub-apertures identically, so can be removed by just subtracting the average tip/tilt across the whole frame, though this also removes any tip/tilt induced from the atmosphere. This tip/tilt also needs to be removed from the theoretical response functions the data is fitted to.

The correlations between the sub-apertures for the different field directions are calculated from theory using Kolmogrov statistics.[10] These correlations then have corrections applied to them for removing the global tip/tilt from

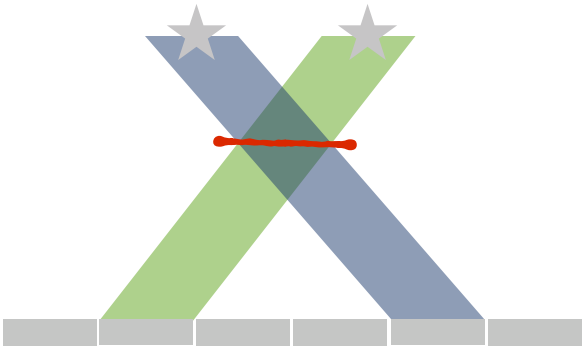

Figure 2. Two sub-apertures looking at two different reference objects (in our case solar granulation) pass through different turbulence. Any correlation between the motion of the granules in the sub-apertures should arise from where they pass through common turbulence. From the correlations between the different lines of sights, and using triangulation it is possible to both determine the height at which the turbulence occurs, as well as its strength. By using many sub-apertures and tracking many different granules (directions), a densely filled atmospheric profile can be generated.

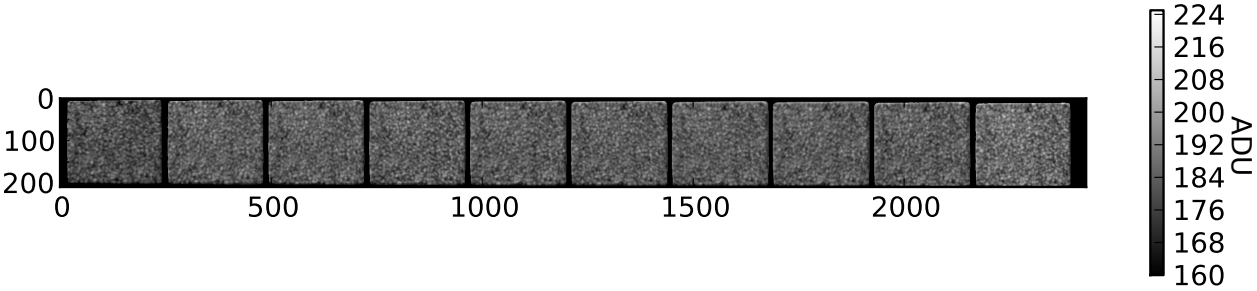


Figure 3. This image shows a processed frame from the WF-WFS, where the x and y axis correspond to pixel number. Each sub-aperture forms a separate image on the camera, with the images lined up as in the shape of the sub-apertures across the pupil. The fields in each of the images is the same, and the differences between the images are due to different turbulence being seen by each of the sub-apertures as they are traced through the atmosphere.

across the telescope pupil, so they match with the data gathered.[11] The expected strength of correlation only depends on the separation of the sub-apertures pointing in different directions, which changes as the sub-apertures are propagated through the atmosphere, as shown in fig 2. The response functions for the instrument are then calculated for a number of different altitudes. This analysis is more akin to SLODAR analysis,[3] rather than the S-DIMM+ analysis that was done previously at the SST.[7] The 37 layers in the profile is greater than a normal SLODAR instrument, which matches the number of layers to the number of sub-apertures across the pupil.[3] This is done as there are many more sources, of different angular separations, available to further constrain the altitude of the turbulence.

Data was gathered for between 45 and 60 seconds at a time, in order to generate a well averaged correlation, to fit to the response functions. The frames are centroided for each sub-aperture, and $7 \times 8$ directions in each of the sub-apertures. These centroids then have their global tip/tilt removed separately for each direction and each frame before being correlated with each other. The profiles are then generated by fitting the measured correlations to the theoretical response functions for different altitudes.

The profiles presented here are still preliminary, as the response functions generated for fitting to the data do not take into account the fact that the centroids are calculated for an extended source. The main effect is the averaging of the turbulence at high layers due to the expanding pupil,[7] meaning the profiles shown here are likely underestimating the strength of the high layer turbulence, as well as working at too high a resolution.

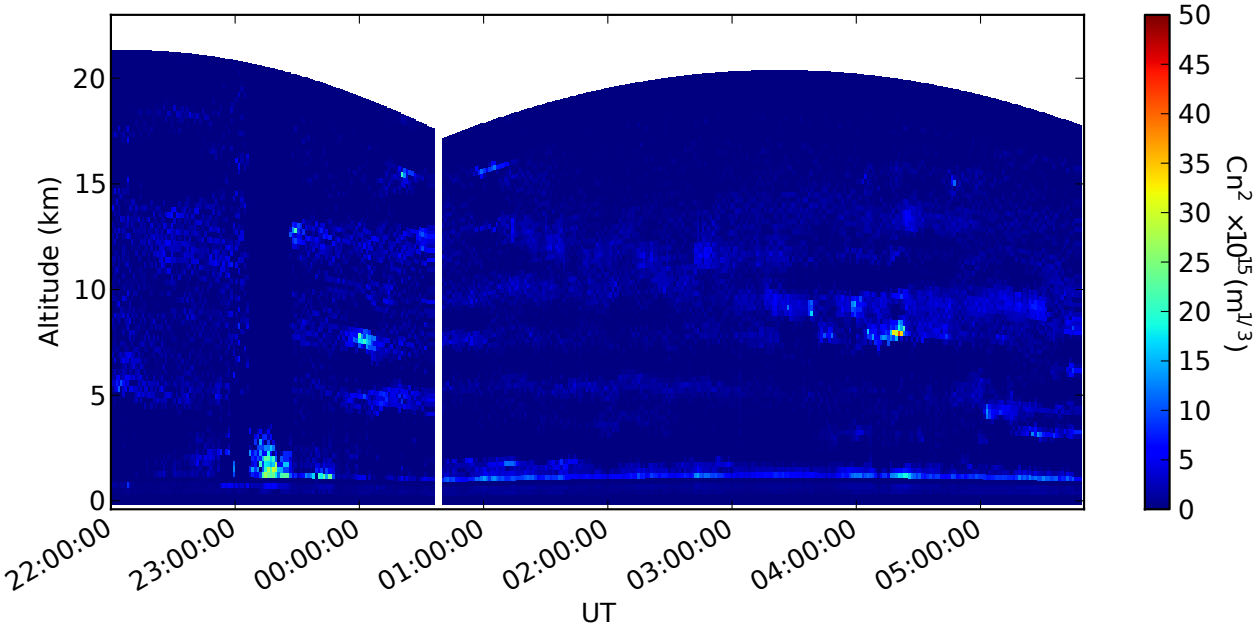


Figure 4. This figure shows the profiles taken on the night of the 18th September 2013 by the Stereo SCIDAR.[9] The instrument switched targets between midnight and 1am where there is an interval in profiles, and a change in the altitude resolution of the instrument. The profiles are high resolution, and it is possible to make out the layers in the atmosphere clearly, as well as being able to see how they evolve over time.

## 3. RESULTS

### 3.1 Nighttime Profiles

The profiles taken by Stereo-SCIDAR from the night of the 18th September 2013 are shown in fig 4. The profiles show definite structure in the turbulence, with distinct layers visible throughout the night, which appear stable. The turbulence seen at the lowest altitude is not physical and a systematic of the system, with no data this altitude. The high altitude turbulence, while being relatively stable does have layers which merge, disappear and reappear throughout the night. The other major thing to note is the strength of the turbulence. The higher altitude turbulence is all of the order of $(1-10) \times 10^{15} m^{1/3}$.

The altitude of the turbulence is scaled to give altitude above the ground, rather than line of sight range. This changes with time as the telescope is tracking an object across the sky, meaning its elevation is constantly changing. This is visible in the top bin as a curve which follows the shape of an airmass function. The line of sight spacing between each of the resolution bins is constant for each of the targets, but when the airmass corrections are applied the apparent altitude of each bin changes by a similar factor, changing the altitude resolution.

### 3.2 Daytime Profiles

The profiles taken during the day on the 19th September 2013 are shown in fig 5. The seeing typically is best during the morning, so observations started at sunrise. The seeing then deteriorates late morning to midday, to such an extent that in the WF-WFS it becomes impossible to see the structure of the solar granulation, rendering data worthless. This was the case for the day shown in fig 5, so the reconstructed profiles stop at 10am, when the seeing began to deteriorate too much.

The fitting typically shows a lot of turbulence in the highest altitude bin. This is not physical and is related to there being more freedom in fitting for higher altitudes. The strength of this layer can be used as an indicator of how good the rest of the fit is, with less strength in the layer suggesting a better fit. The majority of the profiles shown give most of the turbulence close to the ground, with any higher layer turbulence being weak and fairly evenly spread up to around 20km.

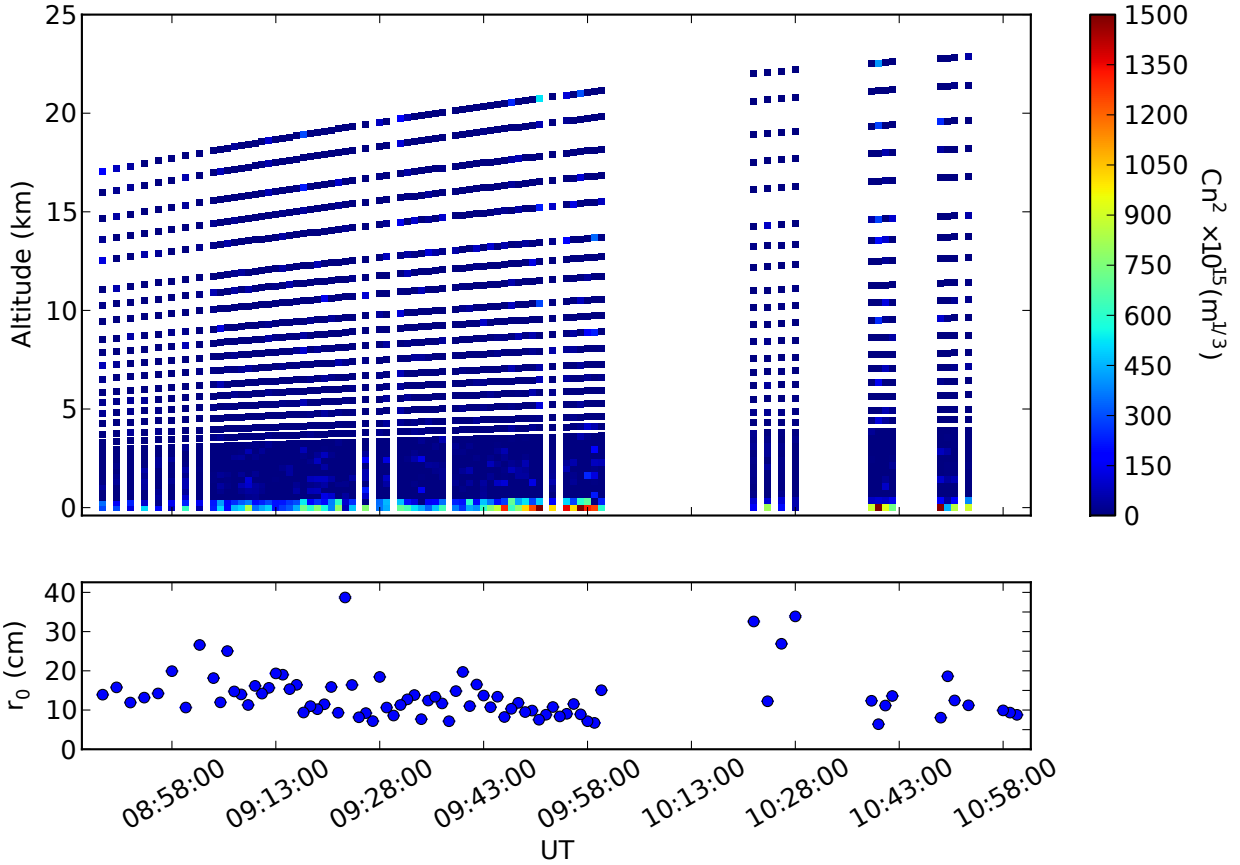


Figure 5. These plots show the atmospheric conditions for the morning of 19th September 2013. The upper plot shows the reconstructed profiles from the WF-WFS, and the lower plot shows the integrated seeing as estimated from the individual image motions of the granules.[12]The turbulence appears mostly at the ground, and the $r_0$ value shows signs of deteriorating towards the end of observations before the images were too poor to continue observing.

Like the nighttime profiles, the day profiles have been corrected for the solar movement across the sky. The total number of altitude bins remains constant, which means that when the sun is close to the horizon the spacing of the bins is small, but the maximum altitude the WF-WFS can see if low, whereas close to zenith the maximum altitude is at its greatest, but the spacing between the bins is also at its largest.

## 4. COMPARISON

The daytime profiles taken in this campaign were compared with those previously taken at the SST by Göran Scharmer, using S-DIMM+.[7] In order to compare these two sets of data the average profile from the 19th September 2013 was taken, then compared to the average profile taken by the S-DIMM+[7] in June 2009. The two profiles can be seen overlaid in the left panel of fig 6. The two profiles have similar shapes, with our data showing more structure to the high layer turbulence, though the resolution is likely to be overestimated.

The average profile from the night profiles is shown alongside the daytime profiles in the right hand plot of fig 6. The average shape of the two profiles seem to be fairly similar. Most of the turbulence located at the ground in the daytime profiles, but unseen in the nighttime profiles. The high altitude turbulence shows some indications of structure in both profiles, but with generally lower altitude turbulence at night.

However the relative strengths of the layers is very different. This is to be expected for the ground layer turbulence, as the solar heating of the ground during the day greatly increases the turbulence there. But the high layer turbulence was expected to be of a more similar strength, though this appears not to be the case, with the strength being much

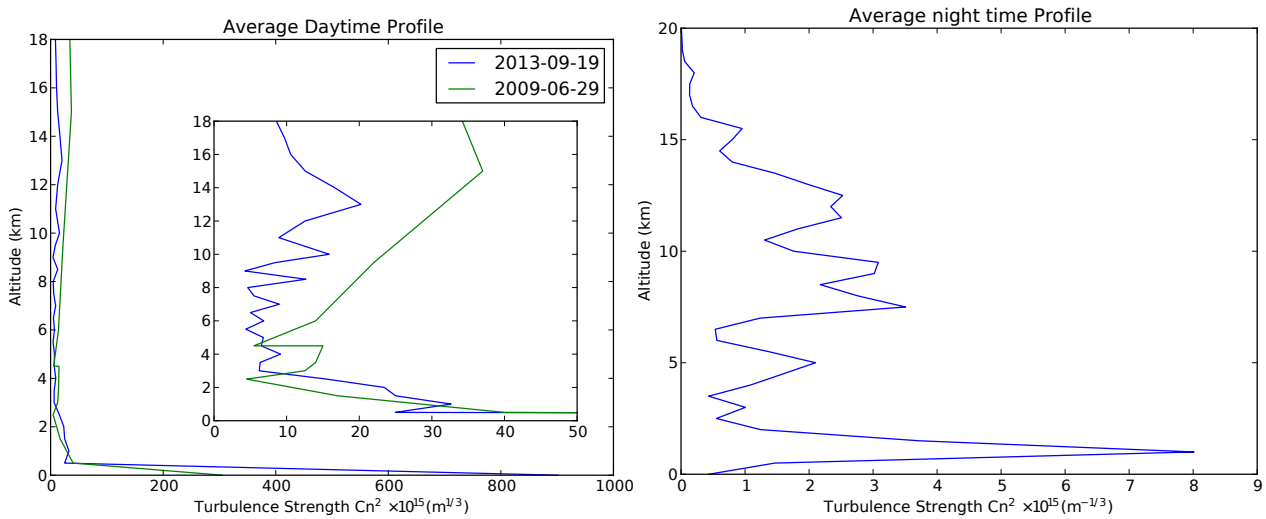


Figure 6. The average daytime profile on the left shows a strong ground layer, and turbulence up to around 25km, mostly continuously. The inserted plot shows the high altitude turbulence in much more detail. So whilst there is high altitude turbulence, it isn't clear that there is any dominant layer responsible. The previously taken profile with the S-DIMM+ also shows a similar structure to this, though at a lower resolution. This suggests that the profiles taken are consistent with each other. The average nighttime profile on the right also shows a strong low altitude layer, which is from systematics, with some relatively strong high layer turbulence, though the general strength of the turbulence is much lower than for the day. The turbulence appears to be lower altitude at night compared to where the turbulence is during the day.

greater during the day than at night. It is not unreasonable to expect this to a certain extent due to general solar heating of the atmosphere during the day.

## 5. CONCLUSION

The amount of data taken during the day for this campaign is relatively small, making it difficult to see any time evolution of the atmosphere throughout the day. So for any kind of analysis of the variability of the atmosphere during the daytime more data would be required. Comparing the average conditions between the night and the day, in fig 6, both the strength and altitude of the turbulence is different. Although there is not enough data here to suggest whether this is representative of the typical conditions.

In order to get better statistics for this analysis, as well as build up enough data to see how turbulence evolves throughout the day, much larger data sets needs to be taken. There are plans to automate the WF-WFS on the SST in order to allow for continuous monitoring of the atmosphere in order to build these extended data sets during the next observing season, 2015.

## ACKNOWLEDGMENTS

The authors would like to thank Peter Sutterlin and Göran Scharmer for all their help and advice, especially at the SST, and the SCIDAR and CANARY teams for their general help both on and off La Palma. M. J. T. gratefully acknowledges support from a UK Science and Technology Facilities Council (STFC) Ph.D studentship (ST/1505656/1), from CANARY for instrument costs (ST/K003569/1) and SCIDAR for their data (UK STFC).

Raw data is available from the lead authors.

## REFERENCES

[1] Hill, F., Beckers, J., Brandt, P., Briggs, J., Brown, T., Brown, W., Collados, M., Denker, C., Fletcher, S., Hegwer, S., Horst, T., Komsa, M., Kuhn, J., Lecinski, A., Lin, H., Oncley, S., Penn, M., Radick, R., Rimmele, T., Socas-Navarro, H., and Streander, K., "Site Testing for the Advanced Technology Solar Telescope," *Proc. SPIE* **6267**, 62671T–62671T–11 (June 2006).

[2] Kellerer, A., Gorceix, N., Marino, J., Cao, W., and Goode, P. R., "Profiles of the daytime atmospheric turbulence above Big Bear solar observatory," *A & A* **542**, A2 (May 2012).

[3] Wilson, R. W., "SLODAR: measuring optical turbulence altitude with a Shack-Hartmann wavefront sensor," *MNRAS* **337**, 103–108 (Nov. 2002).

[4] Vernin, J. and Roddier, F., "Experimental determination of two-dimensional spatiotemporal power spectra of stellar light scintillation Evidence for a multilayer structure of the air turbulence in the upper troposphere," *J. Opt. Soc. Am.* **63**, 270–273 (Mar. 1973).

[5] Beckers, J., Liu, Z., and Jin, Z., "The ATST seeing monitor: February 2002 observations at Fuxian Lake," *Proc. SPIE* **4853**, 273–284 (2002).

[6] Berkefeld, T., Soltau, D., del Moro, D., and Löfdahl, M., "Wavefront Sensing and Wavefront Reconstruction for the 4m European Solar Telescope EST," *Proc. SPIE* **7736**, 77362J–77362J–9 (July 2010).

[7] Scharmer, G. B. and van Werkhoven, T. I. M., "S-DIMM+ height characterization of day-time seeing using solar granulation," *A & A* **513**, A25 (Apr. 2010).

[8] Berkefeld, T., Bettonvil, F., Collados, M., López, R., Martín, Y., Peñate, J., Pérez, A., Scharmer, G. B., Sliepen, G., Soltau, D., Waldmann, T. a., and van Werkhoven, T., "Site-seeing measurements for the European Solar Telescope," *Proc. SPIE* **7733**, 77334I–77334I–10 (July 2010).

[9] Shepherd, H. W., Osborn, J., Wilson, R. W., Butterley, T., Avila, R., Dhillon, V. S., and Morris, T. J., "Stereo-SCIDAR: optical turbulence profiling with high sensitivity using a modified SCIDAR instrument," *MNRAS* **437**, 3568–3577 (Nov. 2014).

[10] Wilson, R. W. and Jenkins, C. R., "Adaptive optics for astronomy: theoretical performance and limitations," *MNRAS* **278**, 39–61 (Jan. 1996).

[11] Butterley, T., Wilson, R. W., and Sarazin, M., "Determination of the profile of atmospheric optical turbulence strength from SLODAR data," *MNRAS* **369**, 835–845 (June 2006).

[12] Sarazin, M. and Roddier, F., "The ESO differential image motion monitor," *A & A* **227**, 294–300 (1990).